

Measurement of the Ω_c^0 Baryon Lifetime

R. Aaij *et al.**
(LHCb Collaboration)

 (Received 5 July 2018; revised manuscript received 31 July 2018; published 31 August 2018)

We report a measurement of the lifetime of the Ω_c^0 baryon using proton-proton collision data at center-of-mass energies of 7 and 8 TeV, corresponding to an integrated luminosity of 3.0 fb^{-1} collected by the LHCb experiment. The sample consists of about 1000 $\Omega_c^- \rightarrow \Omega_c^0 \mu^- \bar{\nu}_\mu X$ signal decays, where the Ω_c^0 baryon is detected in the $pK^-K^-\pi^+$ final state and X represents possible additional undetected particles in the decay. The Ω_c^0 lifetime is measured to be $\tau_{\Omega_c^0} = 268 \pm 24 \pm 10 \pm 2 \text{ fs}$, where the uncertainties are statistical, systematic, and from the uncertainty in the D^+ lifetime, respectively. This value is nearly four times larger than, and inconsistent with, the current world-average value.

DOI: [10.1103/PhysRevLett.121.092003](https://doi.org/10.1103/PhysRevLett.121.092003)

Measurements of the lifetimes of hadrons containing heavy (b or c) quarks play an important role in testing theoretical approaches that are used to predict standard model parameters. The validation of such tools is important, as they can then be used to search for deviations from standard model expectations in other processes. One of the most predictive tools in quark flavor physics is the heavy quark expansion (HQE) [1–8], which describes the decay widths of hadrons containing heavy quarks, Q , through an expansion in powers of $1/m_Q$, where m_Q is the heavy quark mass. While predictions for absolute lifetimes carry relatively large uncertainties, ratios of lifetimes have smaller theoretical uncertainties [9]. Higher-order terms in the HQE are related to nonperturbative corrections, and to effects due to the presence of the other light quark(s) (spectator) in the heavy hadron. For beauty hadrons with a single heavy quark, these corrections are typically at the few percent level or less, due to the large mass of the b quark [9]. For charm hadrons, since m_c is significantly smaller than m_b , these higher-order corrections can be sizable. Therefore measurements of charm-hadron lifetimes provide a sensitive probe of their contributions [10–14].

While charm-meson lifetimes have been measured precisely and provide useful information on these higher-order terms, the knowledge of charm-baryon lifetimes is much less accurate. The lifetimes of the D^0 , D^+ , and D_s^+ mesons are known to about 1% precision, whereas the corresponding uncertainties for the Λ_c^+ , Ξ_c^+ , Ξ_c^0 , and Ω_c^0 baryons are 3%, 6%, 10%, and 17%, respectively [15]. Improved

measurements of the charm-baryon lifetimes provide complementary information to what can be gleaned from charm mesons. For example, contributions from W -exchange and constructive Pauli interference effects are present in charm-baryon decays, but are small or absent in charm-meson decays [11]. Moreover, for charm baryons, the spectator system may have spin 0 (Λ_c^+ , Ξ_c^+ , Ξ_c^0) or spin 1 (Ω_c^0), whereas for charm mesons, the light quark spin is always equal to 1/2.

It has been argued that the expected lifetime hierarchy, due to the higher order contributions discussed above, should be [10–12,16–18]

$$\tau_{\Xi_c^+} > \tau_{\Lambda_c^+} > \tau_{\Xi_c^0} > \tau_{\Omega_c^0}. \quad (1)$$

The quark content of the Ω_c^0 baryon is css , and the qualitative argument that the Ω_c^0 lifetime should be the shortest is predicated on large constructive interference between the s quark in the $c \rightarrow sW^+$ transition in the Ω_c^0 decay and the spectator s quarks in the final state. However, it is also conceivable that the Ω_c^0 lifetime could be the largest, depending on the treatment of higher-order terms in the HQE expansion [12].

Current measurements [15] are consistent with this hierarchy. The least well measured lifetime is that of the Ω_c^0 baryon, with a value of $\tau_{\Omega_c^0} = 69 \pm 12 \text{ fs}$, obtained by fixed-target experiments using a small number of signal decays [19–21].

In this Letter we report a new measurement of the Ω_c^0 baryon lifetime using a sample of semileptonic (SL) $\Omega_b^- \rightarrow \Omega_c^0 \mu^- \bar{\nu}_\mu X$ decays, where the Ω_c^0 baryons are detected in the $pK^-K^-\pi^+$ final state and X represents any additional undetected particles. Semileptonic b -meson decays were used previously by LHCb to make precise measurements of the D_s^+ and B_s^0 lifetimes [22]. Throughout the text, charge-conjugate processes are implicitly included.

*Full author list given at the end of the article.

Published by the American Physical Society under the terms of the [Creative Commons Attribution 4.0 International license](https://creativecommons.org/licenses/by/4.0/). Further distribution of this work must maintain attribution to the author(s) and the published article's title, journal citation, and DOI. Funded by SCOAP³.

To reduce the uncertainties associated with systematic effects, the lifetime ratio

$$r_{\Omega_c^0} \equiv \frac{\tau_{\Omega_c^0}}{\tau_{D^+}} \quad (2)$$

is measured, where the D^+ meson is detected in $B \rightarrow D^+ \mu^- \bar{\nu}_\mu X$ decays, with $D^+ \rightarrow K^- \pi^+ \pi^+$. In the following, the symbols H_b and H_c are used to refer to the b or c hadron in either of the two modes indicated above.

The measurement uses proton-proton (pp) collision data samples, collected by the LHCb experiment, corresponding to an integrated luminosity of 3.0 fb^{-1} , of which 1.0 fb^{-1} was recorded at a center-of-mass energy of 7 TeV and 2.0 fb^{-1} at 8 TeV. The LHCb detector [23,24] is a single-arm forward spectrometer covering the pseudorapidity range $2 < \eta < 5$, designed for the study of particles containing b or c quarks. The tracking system provides a measurement of momentum p of charged particles with a relative uncertainty that varies from 0.5% at low momentum to 1.0% at 200 GeV/ c . The minimum distance of a track to a primary vertex (PV), the impact parameter (IP), is measured with a resolution of $(15 + 29/p_T) \mu\text{m}$, where p_T is the component of the momentum transverse to the beam, in GeV/ c . Charged hadrons are identified using information from two ring-imaging Cherenkov (RICH) detectors [25]. Muons are identified by a system composed of alternating layers of iron and multiwire proportional chambers [26]. The online event selection is performed by a trigger [27], which consists of a hardware stage, based on information from the calorimeter and muon systems, followed by a software stage, which applies a full event reconstruction.

Simulation is required to model the effects of the detector acceptance and the imposed selection requirements. Proton-proton collisions are simulated using PYTHIA [28] with a specific LHCb configuration [29]. Decays of hadronic particles are described by EVTGEN [30], in which final-state radiation is generated using PHOTOS [31]. The interaction of the generated particles with the detector and its response are implemented using the GEANT4 toolkit [32] as described in Ref. [33].

Signal Ω_b^- candidates are formed by combining an $\Omega_c^0 \rightarrow pK^-K^- \pi^+$ candidate with a μ^- candidate. Each final-state particle in the decay is required to be detached from all PVs in the event, and is associated to the one with the smallest χ_{IP}^2 . Here, χ_{IP}^2 is defined as the difference in χ^2 of the particle's associated PV reconstructed with and without the considered track. The muon is required to have $p_T > 1 \text{ GeV}/c$, $p > 6 \text{ GeV}/c$ and have particle identification (PID) information consistent with being a muon. The Ω_c^0 candidate's decay products must have PID information consistent with their assumed particle hypotheses, and have $p_T > 0.25 \text{ GeV}/c$ and $p > 2 \text{ GeV}/c$, except for the proton, which is required to have

$p > 8 \text{ GeV}/c$. To remove the contribution from promptly produced Ω_c^0 baryons, each Ω_c^0 candidate's reconstructed trajectory must not point back to any PV in the event. Only Ω_c^0 candidates that have an invariant mass within $60 \text{ MeV}/c^2$ of the known Ω_c^0 mass are retained.

The $\Omega_c^0 \mu^-$ combinations are required to form a good quality vertex and satisfy the invariant mass requirement, $m(\Omega_c^0 \mu^-) < 8.0 \text{ GeV}/c^2$. Random combinations of Ω_c^0 and μ^- are suppressed by requiring the fitted z coordinates of the Ω_c^0 and Ω_b^- decay vertices to satisfy $z(\Omega_c^0) - z(\Omega_c^0 \mu^-) > -0.05 \text{ mm}$, where the z axis is parallel to the beam direction.

To ensure precise modeling of the decay-time acceptance from simulation, the candidates must satisfy a well-defined set of hardware and software trigger requirements. At the hardware level, candidates are required to pass the single-muon trigger, and, at the software level, to pass specific triggers designed to select multi-body final states containing a muon [27].

To improve the signal-to-background ratio in the $\Omega_c^0 \mu^-$ sample, a boosted decision tree (BDT) discriminant [34,35] is built from 18 variables, which include the χ^2 for the Ω_b^- and Ω_c^0 decay-vertex fits, and χ_{IP}^2 , p , p_T , and a PID response variable for each final-state hadron. The BDT is trained using simulated $\Omega_b^- \rightarrow \Omega_c^0 \mu^- \bar{\nu}_\mu X$ decays for the signal, while background is taken from the Ω_c^0 mass sidebands, $30 < |m(pK^-K^- \pi^+) - m_{\Omega_c^0}| < 50 \text{ MeV}/c^2$, where $m_{\Omega_c^0}$ is the known Ω_c^0 mass [15]. The requirement on the BDT response is determined by optimizing the figure of merit $S/\sqrt{S+B}$, where S and B are the expected signal and background yields within a $\pm 15 \text{ MeV}/c^2$ mass region centered on the mass peak, respectively. The optimal BDT requirement provides a signal (background) efficiency of 78% (16%).

The $D^+ \mu^-$ candidates, used for normalization, are formed by combining $D^+ \rightarrow K^- \pi^+ \pi^+$ and μ^- candidates. The selections are identical to those discussed above, except the mass window is centered on the known D^+ mass and the BDT requirement is eliminated. Only 10% of the $D^+ \mu^-$ data, selected at random, are used in the analysis, since the full sample is much larger than needed for this measurement.

The invariant-mass distributions for the selected Ω_c^0 and D^+ candidates in the two $H_c \mu^-$ final states are shown in Fig. 1. Both distributions are fitted using the sum of a signal component, defined as the sum of two Gaussian functions with a common mean, and an exponential shape to represent the combinatorial background. From a binned maximum-likelihood fit, the fitted $\Omega_c^0 \mu^-$ and $D^+ \mu^-$ yields are 978 ± 60 and $(809 \pm 1) \times 10^3$, respectively. The number of Ω_c^0 signal decays is at least an order of magnitude larger than any previous sample used for an Ω_c^0 lifetime measurement.

The decay time of each H_c candidate is determined from the positions of the H_b and H_c decay vertices, and

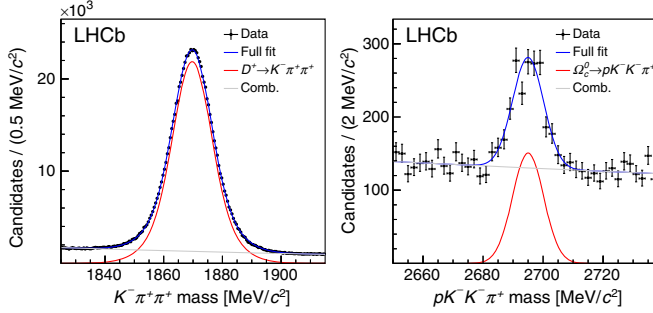


FIG. 1. Invariant-mass distributions for (left) D^+ candidates in $B \rightarrow D^+ \mu^- \bar{\nu}_\mu X$ decays and (right) Ω_c^0 candidates in $\Omega_c^0 \mu^- \bar{\nu}_\mu X$ decays. The results of the fits, as described in the text, are overlaid.

the measured H_c momentum. The background-subtracted decay-time spectra are obtained using the *sPlot* technique [36], where the measured H_c mass is used as the discriminating variable. The uncertainties in the bin-by-bin signal yields reflect both the finite signal yield and the statistical uncertainty due to the background subtraction.

Potential backgrounds from (i) random $H_c \mu^-$ combinations, (ii) $H_b \rightarrow H_c \tau^- \bar{\nu}_\tau$, $\tau^- \rightarrow \mu^- \nu_\tau \bar{\nu}_\mu$ decays, and (iii) $H_b \rightarrow H_c \bar{D}$, $\bar{D} \rightarrow \mu^- X$, where \bar{D} represents a D_s^- , D^- or \bar{D}^0 meson, could lead to a bias on the lifetime, since the muon is not produced directly at the H_b decay vertex. These backgrounds have been investigated and constitute a small fraction of the observed signal, about 3% in total, and have decay-time spectra that are similar to the true $H_c \mu^- \bar{\nu}_\mu$ final state due to the χ^2 requirements on the H_b vertex fit. Moreover, these backgrounds affect the signal and the normalization mode similarly, thus leading to at least a partial cancellation of any bias. Contamination in the $\Omega_c^0 \mu^- \bar{\nu}_\mu X$ sample from misidentified four-body D^0 final states in $B \rightarrow D^0 \mu^- \bar{\nu}_\mu X$ decays has been investigated, and none are found to peak in the Ω_c^0 signal region.

The decay-time spectra for the Ω_c^0 and D^+ signals are shown in Fig. 2, along with the results of the fits described below. The decrease in the signal yield as the decay time approaches zero is mainly due to the effects of the H_c decay-time resolution, which is in the range of 85–100 fs, and the $z(H_c) - z(H_c \mu^-) > -0.05$ mm requirement.

The decay-time signal model $S(t_{\text{rec}})$ takes the form

$$S(t_{\text{rec}}) = f(t_{\text{rec}})g(t_{\text{rec}})\beta(t_{\text{rec}}). \quad (3)$$

Here, $f(t_{\text{rec}})$ is a signal template of reconstructed decay times, obtained from the full LHCb simulation, after all selections have been applied as in the data. The signal template is multiplied by $g(t_{\text{rec}}) = \exp(-t_{\text{rec}}/\tau_{\text{fit}}^{H_c}) / \exp(-t_{\text{rec}}/\tau_{\text{sim}}^{H_c})$, where $\tau_{\text{sim}}^{D^+} = 1040$ fs and $\tau_{\text{sim}}^{\Omega_c^0} = 250$ fs are the lifetimes used in the simulation, and $\tau_{\text{fit}}^{H_c}$ is the signal lifetime to be fitted. The function $\beta(t_{\text{rec}})$ is a correction that

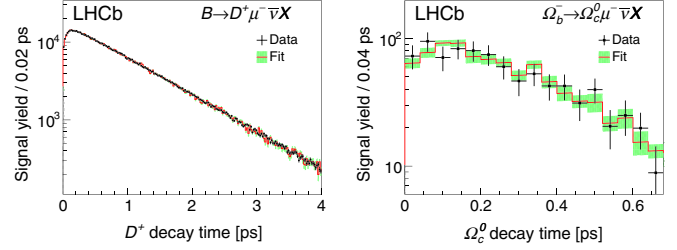


FIG. 2. Decay-time spectra for (left) D^+ signal in $B \rightarrow D^+ \mu^- \bar{\nu}_\mu X$ events and (right) Ω_c^0 signal in $\Omega_c^0 \mu^- \bar{\nu}_\mu X$ events. Overlaid are the fit results, as described in the text, along with the uncertainties due to finite simulated sample sizes.

accounts for a small difference in the efficiency between data and simulation for reconstructing tracks in the vertex detector that originate far from the beam line [37].

Given the precise knowledge of the D^+ meson lifetime (1040 ± 7 fs) [15], the $D^+ \mu^-$ sample is used to calibrate $\beta(t_{\text{rec}})$ and validate the fit. The signal template is obtained from simulated $B \rightarrow D^+ \mu^- \bar{\nu}_\mu X$ decays, where contributions from $B \rightarrow D^+ \tau^- \bar{\nu}_\tau X$ decays are included. The function $\beta(t_{\text{rec}})$ is obtained by taking the ratio between the D^+ decay-time spectrum in data (obtained via the *sPlot* technique) and that obtained from simulation. The ratio shows a linear dependence, and a fit to the function $\beta(t_{\text{rec}}) = 1 + \beta_0 t_{\text{rec}}$ yields $\beta_0 = (-0.89 \pm 0.32) \times 10^{-2} \text{ ps}^{-1}$. If the $\beta(t_{\text{rec}})$ function is excluded from the fit, $\tau_{\text{fit}}^{D^+}$ is 10 fs below the world average. The result of the binned χ^2 fit after this correction is applied is shown in Fig. 2 (left), where the fitted lifetime is found to be $\tau_{\text{fit}}^{D^+} = 1042.0 \pm 1.7(\text{stat})$ fs.

The Ω_c^0 lifetime is determined from a simultaneous fit to the Ω_c^0 and D^+ decay-time spectra, for which the free parameters in the fit are $r_{\Omega_c^0}$ [see Eq. (2)] and $\tau_{\text{fit}}^{D^+}$. By fitting for the ratio $r_{\Omega_c^0}$, correlated systematic uncertainties partially cancel. In the Ω_c^0 decay-time fit, β_0 is scaled by 4/3 since the effect is expected to scale with the number of charged final state particles in the H_c decay [37]. The simulation includes contributions from $\Omega_c^0 \tau^- \bar{\nu}_\tau X$ final states. The results of the fit to the Ω_c^0 decay-time distribution are shown in Fig. 2 (right), where the value $r_{\Omega_c^0} = 0.258 \pm 0.023(\text{stat})$ is obtained. Multiplying this value by $\tau^{D^+} = 1040$ fs [15], the Ω_c^0 lifetime is measured to be 268 ± 24 fs. This is about four times larger than, and incompatible with, the current world average value of 69 ± 12 fs [15].

Several cross-checks have been performed to ensure the robustness of this result. To confirm that the signal events are from SL Ω_c^0 decays, a number of distributions, such as the $\Omega_c^0 \mu^-$ mass spectrum, p_T and decay time have been compared between data (using *sPlot*) and the $\Omega_c^0 \mu^- \bar{\nu}_\mu X$ simulation. In all cases, good agreement is found. The lifetime measurement has also been performed using a

simple subtraction of the Ω_c^0 mass sidebands, and we find good agreement with the value obtained by the *sPlot* technique. The Ω_c^0 decay-time distribution obtained from an independent and comparably sized data sample of semileptonic decays collected at 13 TeV center-of-mass energy has been examined, and the distribution is consistent with the one observed here. The procedure has also been checked using a sample of about 88 000 $B^- \rightarrow D^0(\rightarrow K^+ K^- \pi^+ \pi^-) \mu^- X$ decays to measure the D^0 meson lifetime. The obtained lifetime is consistent with the expected value within about one standard deviation. The analysis has also been carried out with either tighter PID or tighter BDT requirements, and the fitted Ω_c^0 lifetime in each case is consistent with the value from the default fit. The analysis has also been checked with the Λ_c^+ baryon, and the lifetime is consistent with expectations.

A number of sources of systematic uncertainty on the measured ratio $r_{\Omega_c^0}$ have been investigated, and are summarized in Table I. The decay time acceptance correction $\beta(t_{\text{rec}})$ leads to an uncertainty of 0.5% on $r_{\Omega_c^0}$, which includes a contribution from the finite sample sizes and the choice of fit function.

Studies of the D^+ calibration mode show a small dependence of the β_0 parameter on the p_T and η of the H_b hadron. In the case that the p_T and η spectra in data and simulation differ, it could cause a shift in the average β_0 . The uncertainty on $r_{\Omega_c^0}$ is obtained by taking into account the variation of β_0 in different p_T and η ranges, and the extent to which the p_T and η spectra may differ between data and simulation.

The world-average value of the Ω_b^- lifetime is $1.64_{-0.17}^{+0.18}$ ps [15], whereas the simulation uses 1.60 ps. To assess the potential impact on the Ω_c^0 lifetime, we weight $f(t_{\text{rec}})$ to replicate an Ω_b^- lifetime of either 1.50 or 1.70 ps. The changes in $r_{\Omega_c^0}$ are assigned as a systematic uncertainty.

The decay-time resolution has been checked by comparing the D^0 decay-time spectra in $B^- \rightarrow D^0 \pi^-$ decays, where no explicit requirement on the flight distance of the D^0 is applied. Negative decay times are entirely due to

the decay-time resolution, and simulation is found to agree well with data. To assess a potential impact of a small difference in decay-time resolution between simulation and data, new Ω_c^0 and D^+ signal templates are formed where the reconstructed decay time is smeared by an additional 15%, beyond what is produced by the full simulation. The fit is redone, and the difference in $r_{\Omega_c^0}$ from the nominal value is assigned as a systematic uncertainty.

The method for background subtraction uses the *sPlot* technique, which has some dependence on the choice of signal and background functions. To assess a potential systematic effect, the decay-time spectra are obtained using a sideband subtraction of the H_c mass spectra for both the signal and the normalization modes. The sideband-subtracted decay-time spectra are then fitted using the decay-time fit described above. The difference between this result and the nominal one is assigned as a systematic uncertainty.

The decay-time spectra in both $\Omega_c^0 \mu^-$ and $D^+ \mu^-$ samples have small contributions from random combinations of H_c and μ^- candidates [(0.8 ± 0.2)% of the signal], as well as physics backgrounds where the μ^- comes from either a τ^- [(1.8 ± 0.3)%] or a SL D decay [(0.5 ± 0.2)%]. From simulation and data control samples, we find that the effective lifetimes of these backgrounds are within 10% of the true signal lifetime; this is due to the requirement that the muon candidate must form a good vertex with the H_c candidate. The impact on the Ω_c^0 lifetime is evaluated using pseudoexperiments, where mixtures of these backgrounds (with different decay-time spectra) and signal decays are formed and fitted assuming a single lifetime for the sample. The difference in the mean value of $r_{\Omega_c^0}$ between the nominal fit, and that with the backgrounds added is assigned as the systematic uncertainty.

The systematic uncertainty due to the finite size of the simulated samples is assessed by repeating the fit to the data many times, where in each fit the simulated-template bin contents are fluctuated within their uncertainties. The standard deviation of the distribution of the fitted $r_{\Omega_c^0}$ values is assigned as a systematic uncertainty.

In summary, we use pp collision data samples at 7 and 8 TeV center-of-mass energies, corresponding to 3.0 fb⁻¹ of integrated luminosity, to measure the lifetime of the Ω_c^0 baryon. The measured ratio of lifetimes and absolute Ω_c^0 lifetime are

$$\begin{aligned} \frac{\tau_{\Omega_c^0}}{\tau_{D^+}} &= 0.258 \pm 0.023 \pm 0.010, \\ \tau_{\Omega_c^0} &= 268 \pm 24 \pm 10 \pm 2 \text{ fs}, \end{aligned}$$

where the first uncertainty is statistical, the second is systematic, and the third is due to the uncertainty in the D^+ lifetime [15]. The measured Ω_c^0 lifetime is about four times larger than, and inconsistent with, the world average value of 69 ± 12 fs [15].

TABLE I. Summary of systematic uncertainties on the lifetime ratio, $r_{\Omega_c^0}$, in units of 10^{-4} .

Source	$r_{\Omega_c^0}$ (10^{-4})
Decay-time acceptance	13
Ω_b^- production spectrum	3
Ω_b^- lifetime	4
Decay-time resolution	3
Background subtraction	18
$H_c(\tau^-, D)$, random μ^-	8
Simulated sample size	98
Total systematic	101
Statistical uncertainty	230

With this measurement, the lifetime hierarchy places the Ω_c^0 baryon as having the second largest lifetime after the Ξ_c^+ baryon,

$$\tau_{\Xi_c^+} > \tau_{\Omega_c^0} > \tau_{\Lambda_c^+} > \tau_{\Xi_c^0}.$$

The result presented here may suggest that the constructive interference between the s quark in the $c \rightarrow sW^+$ transition in the Ω_c^0 decay and the spectator s quarks in the final state is smaller than expected, that the spin of the ss system plays a larger role, or that additional or higher order contributions in the heavy quark expansion need to be considered.

We express our gratitude to our colleagues in the CERN accelerator departments for the excellent performance of the LHC. We thank the technical and administrative staff at the LHCb institutes. We acknowledge support from CERN and from the national agencies: CAPES, CNPq, FAPERJ and FINEP (Brazil); MOST and NSFC (China); CNRS/IN2P3 (France); BMBF, DFG and MPG (Germany); INFN (Italy); NWO (Netherlands); MNiSW and NCN (Poland); MEN/IFA (Romania); MinES and FASO (Russia); MinECo (Spain); SNSF and SER (Switzerland); NASU (Ukraine); STFC (United Kingdom); NSF (USA). We acknowledge the computing resources that are provided by CERN, IN2P3 (France), KIT and DESY (Germany), INFN (Italy), SURF (Netherlands), PIC (Spain), GridPP (United Kingdom), RRCKI and Yandex LLC (Russia), CSCS (Switzerland), IFIN-HH (Romania), CBPF (Brazil), PL-GRID (Poland) and OSC (USA). We are indebted to the communities behind the multiple open-source software packages on which we depend. Individual groups or members have received support from AvH Foundation (Germany); EPLANET, Marie Skłodowska-Curie Actions and ERC (European Union); ANR, Labex P2IO and OCEVU, and Région Auvergne-Rhône-Alpes (France); Key Research Program of Frontier Sciences of CAS, CAS PIFI, and the Thousand Talents Program (China); RFBR, RSF and Yandex LLC (Russia); GVA, XuntaGal and GENCAT (Spain); Herchel Smith Fund, the Royal Society, the English-Speaking Union and the Leverhulme Trust (United Kingdom); Laboratory Directed Research and Development program of LANL (USA).

[1] V. A. Khoze and M. A. Shifman, Heavy quarks, *Sov. Phys. Usp.* **26**, 387 (1983).
 [2] I. I. Y. Bigi and N. G. Uraltsev, Gluonic enhancements in non-spectator beauty decays—an inclusive mirage though an exclusive possibility, *Phys. Lett. B* **280**, 271 (1992).
 [3] I. I. Bigi, N. G. Uraltsev, and A. I. Vainshtein, Nonperturbative corrections to inclusive beauty and charm decays: QCD versus phenomenological models, *Phys. Lett. B* **293**, 430 (1992); Erratum, *Phys. Lett. B* **297**, 477(E) (1992).
 [4] B. Blok and M. Shifman, The rule of discarding $1/N_c$ in inclusive weak decays (I), *Nucl. Phys.* **B399**, 441 (1993).

[5] B. Blok and M. Shifman, The rule of discarding $1/N_c$ in inclusive weak decays (II), *Nucl. Phys.* **B399**, 459 (1993).
 [6] M. Neubert, B decays and the heavy quark expansion, *Adv. Ser. Dir. High Energy Phys.* **15**, 239 (1998).
 [7] N. Uraltsev, Heavy quark expansion in beauty and its decays, [arXiv:hep-ph/9804275](https://arxiv.org/abs/hep-ph/9804275); also published in *Proceedings, Heavy Flavour Physics: A Probe of Nature's Grand Design, Proc. Intern. School of Physics "Enrico Fermi," Course CXXXVII*, edited by I. Bigi and L. Moroni (IOS Press, Amsterdam, 1998).
 [8] I. I. Bigi, The QCD perspective on lifetimes of heavy flavor hadrons, [arXiv:hep-ph/9508408](https://arxiv.org/abs/hep-ph/9508408).
 [9] A. Lenz, Lifetimes and heavy quark expansion, *Int. J. Mod. Phys. A* **30**, 1543005 (2015).
 [10] H.-Y. Cheng, Charmed baryons circa 2015, *Front. Phys. (Beijing)* **10**, 101406 (2015).
 [11] S. Bianco, F. L. Fabbri, D. Benson, and I. Bigi, A cicerone for the physics of charm, *Riv. Nuovo Cimento* **26N7**, 1 (2003).
 [12] B. Blok and M. A. Shifman, Lifetimes of charmed hadrons revisited. Facts and fancy, [arXiv:hep-ph/9311331](https://arxiv.org/abs/hep-ph/9311331).
 [13] M. Kirk, A. Lenz, and T. Rauh, Dimension-six matrix elements for meson mixing and lifetimes from sum rules, *J. High Energy Phys.* **12** (2017) 068.
 [14] A. Lenz and T. Rauh, D-meson lifetimes within the heavy quark expansion, *Phys. Rev. D* **88**, 034004 (2013).
 [15] M. Tanabashi *et al.* (Particle Data Group), Review of particle physics, *Phys. Rev. D* **98**, 030001 (2018).
 [16] H.-Y. Cheng, A phenomenological analysis of heavy hadron lifetimes, *Phys. Rev. D* **56**, 2783 (1997).
 [17] G. Bellini, I. I. Y. Bigi, and P. J. Dornan, Lifetimes of charm and beauty hadrons, *Phys. Rep.* **289**, 1 (1997).
 [18] M. A. Shifman and M. B. Voloshin, Preasymptotic effects in inclusive weak decays of charmed particles, *Yad. Fiz.* **41**, 187 (1985) [*Sov. J. Nucl. Phys.* **41**, 120 (1985)].
 [19] J. M. Link *et al.* (FOCUS Collaboration), Measurement of the Ω_c^0 lifetime, *Phys. Lett. B* **561**, 41 (2003).
 [20] M. I. Adamovich *et al.* (WA89 Collaboration), Measurement of the Ω_c^0 lifetime, *Phys. Lett. B* **358**, 151 (1995).
 [21] P. L. Frabetti *et al.* (E687 Collaboration), First measurement of the lifetime of the Ω_c^0 , *Phys. Lett. B* **357**, 678 (1995).
 [22] R. Aaij *et al.* (LHCb Collaboration), Measurement of B_s^0 and D_s^- Meson Lifetimes, *Phys. Rev. Lett.* **119**, 101801 (2017).
 [23] A. A. Alves Jr. *et al.* (LHCb Collaboration), The LHCb detector at the LHC, *J. Instrum.* **3**, S08005 (2008).
 [24] R. Aaij *et al.* (LHCb Collaboration), LHCb detector performance, *Int. J. Mod. Phys. A* **30**, 1530022 (2015).
 [25] M. Adinolfi *et al.*, Performance of the LHCb RICH detector at the LHC, *Eur. Phys. J. C* **73**, 2431 (2013).
 [26] F. Archilli *et al.*, Performance of the muon identification at LHCb, *J. Instrum.* **8**, P10020 (2013).
 [27] R. Aaij *et al.*, The LHCb trigger and its performance in 2011, *J. Instrum.* **8**, P04022 (2013).
 [28] T. Sjöstrand, S. Mrenna, and P. Skands, PYTHIA 6.4 physics and manual, *J. High Energy Phys.* **05** (2006) 026; A brief introduction to PYTHIA 8.1, *Comput. Phys. Commun.* **178**, 852 (2008).

- [29] I. Belyaev *et al.*, Handling of the generation of primary events in Gauss, the LHCb simulation framework, *J. Phys. Conf. Ser.* **331**, 032047 (2011).
- [30] D. J. Lange, The EvtGen particle decay simulation package, *Nucl. Instrum. Methods Phys. Res., Sect. A* **462**, 152 (2001).
- [31] P. Golonka and Z. Was, PHOTOS Monte Carlo: A precision tool for QED corrections in Z and W decays, *Eur. Phys. J. C* **45**, 97 (2006).
- [32] J. Allison *et al.* (Geant4 Collaboration), Geant4 developments and applications, *IEEE Trans. Nucl. Sci.* **53**, 270 (2006); S. Agostinelli *et al.* (Geant4 Collaboration), Geant4: A simulation toolkit, *Nucl. Instrum. Methods Phys. Res., Sect. A* **506**, 250 (2003).
- [33] M. Clemencic, G. Corti, S. Easo, C. R. Jones, S. Miglioranza, M. Pappagallo, and P. Robbe, The LHCb simulation application, Gauss: Design, evolution and experience, *J. Phys. Conf. Ser.* **331**, 032023 (2011).
- [34] L. Breiman, J. H. Friedman, R. A. Olshen, and C. J. Stone, *Classification and Regression Trees* (Wadsworth International Group, Belmont, 1984).
- [35] Y. Freund and R. E. Schapire, A decision-theoretic generalization of on-line learning and an application to boosting, *J. Comput. Syst. Sci.* **55**, 119 (1997).
- [36] M. Pivk and F. R. Le Diberder, sPlot: A statistical tool to unfold data distributions, *Nucl. Instrum. Methods* **A555**, 356 (2005).
- [37] R. Aaij *et al.* (LHCb Collaboration), Measurements of the B^+ , B^0 , B_s^0 meson and Λ_b^0 baryon lifetimes, *J. High Energy Phys.* **04** (2014) 114.

R. Aaij,²⁷ B. Adeva,⁴¹ M. Adinolfi,⁴⁸ C. A. Aidala,⁷³ Z. Ajaltouni,⁵ S. Akar,⁵⁹ P. Albicocco,¹⁸ J. Albrecht,¹⁰ F. Alessio,⁴² M. Alexander,⁵³ A. Alfonso Alberro,⁴⁰ S. Ali,²⁷ G. Alkhazov,³³ P. Alvarez Cartelle,⁵⁵ A. A. Alves Jr.,⁴¹ S. Amato,² S. Amerio,²³ Y. Amhis,⁷ L. An,³ L. Anderlini,¹⁷ G. Andreassi,⁴³ M. Andreotti,^{16,a} J. E. Andrews,⁶⁰ R. B. Appleby,⁵⁶ F. Archilli,²⁷ P. d'Argent,¹² J. Arnau Romeu,⁶ A. Artamonov,³⁹ M. Artuso,⁶¹ K. Arzymatov,³⁷ E. Aslanides,⁶ M. Atzeni,⁴⁴ B. Audurier,²² S. Bachmann,¹² J. J. Back,⁵⁰ S. Baker,⁵⁵ V. Balagura,^{7,b} W. Baldini,¹⁶ A. Baranov,³⁷ R. J. Barlow,⁵⁶ S. Barsuk,⁷ W. Barter,⁵⁶ F. Baryshnikov,⁷⁰ V. Batozskaya,³¹ B. Batsukh,⁶¹ V. Battista,⁴³ A. Bay,⁴³ J. Beddow,⁵³ F. Bedeschi,²⁴ I. Bediaga,¹ A. Beiter,⁶¹ L. J. Bel,²⁷ S. Belin,²² N. Belyi,⁶³ V. Bellee,⁴³ N. Belloli,^{20,c} K. Belous,³⁹ I. Belyaev,^{34,42} E. Ben-Haim,⁸ G. Bencivenni,¹⁸ S. Benson,²⁷ S. Beranek,⁹ A. Berezhnoy,³⁵ R. Bernet,⁴⁴ D. Berninghoff,¹² E. Bertholet,⁸ A. Bertolin,²³ C. Betancourt,⁴⁴ F. Betti,^{15,42} M. O. Bettler,⁴⁹ M. van Beuzekom,²⁷ I. A. Bezshyiko,⁴⁴ S. Bhasin,⁴⁸ J. Bhom,²⁹ S. Bifani,⁴⁷ P. Billoir,⁸ A. Birmkrant,¹⁰ A. Bizzeti,^{17,d} M. Bjørn,⁵⁷ M. P. Blago,⁴² T. Blake,⁵⁰ F. Blanc,⁴³ S. Blusk,⁶¹ D. Bobulska,⁵³ V. Bocci,²⁶ O. Boente Garcia,⁴¹ T. Boettcher,⁵⁸ A. Bondar,^{38,e} N. Bondar,³³ S. Borghi,^{56,42} M. Borisyak,³⁷ M. Borsato,⁴¹ F. Bossu,⁷ M. Boubdir,⁹ T. J. V. Bowcock,⁵⁴ C. Bozzi,^{16,42} S. Braun,¹² M. Brodski,⁴² J. Brodzicka,²⁹ A. Brossa Gonzalo,⁵⁰ D. Brundu,²² E. Buchanan,⁴⁸ A. Buonaura,⁴⁴ C. Burr,⁵⁶ A. Bursche,²² J. Buytaert,⁴² W. Byczynski,⁴² S. Cadeddu,²² H. Cai,⁶⁴ R. Calabrese,^{16,a} R. Calladine,⁴⁷ M. Calvi,^{20,c} M. Calvo Gomez,^{40,f} A. Camboni,^{40,f} P. Campana,¹⁸ D. H. Campora Perez,⁴² L. Capriotti,⁵⁶ A. Carbone,^{15,g} G. Carboni,²⁵ R. Cardinale,^{19,h} A. Cardini,²² P. Carniti,^{20,c} L. Carson,⁵² K. Carvalho Akiba,² G. Casse,⁵⁴ L. Cassina,²⁰ M. Cattaneo,⁴² G. Cavallero,^{19,h} R. Cenci,^{24,i} D. Chamont,⁷ M. G. Chapman,⁴⁸ M. Charles,⁸ Ph. Charpentier,⁴² G. Chatzikonstantinidis,⁴⁷ M. Chefdeville,⁴ V. Chekalina,³⁷ C. Chen,³ S. Chen,²² S.-G. Chitic,⁴² V. Chobanova,⁴¹ M. Chruszcz,⁴² A. Chubykin,³³ P. Ciambone,¹⁸ X. Cid Vidal,⁴¹ G. Ciezarek,⁴² P. E. L. Clarke,⁵² M. Clemencic,⁴² H. V. Cliff,⁴⁹ J. Closier,⁴² V. Coco,⁴² J. A. B. Coelho,⁷ J. Cogan,⁶ E. Cogneras,⁵ L. Cojocariu,³² P. Collins,⁴² T. Colombo,⁴² A. Comerma-Montells,¹² A. Contu,²² G. Coombs,⁴² S. Coquereau,⁴⁰ G. Corti,⁴² M. Corvo,^{16,a} C. M. Costa Sobral,⁵⁰ B. Couturier,⁴² G. A. Cowan,⁵² D. C. Craik,⁵⁸ A. Crocombe,⁵⁰ M. Cruz Torres,¹ R. Currie,⁵² C. D'Ambrosio,⁴² F. Da Cunha Marinho,² C. L. Da Silva,⁷⁴ E. Dall'Occo,²⁷ J. Dalseno,⁴⁸ A. Danilina,³⁴ A. Davis,³ O. De Aguiar Francisco,⁴² K. De Bruyn,⁴² S. De Capua,⁵⁶ M. De Cian,⁴³ J. M. De Miranda,¹ L. De Paula,² M. De Serio,^{14,j} P. De Simone,¹⁸ C. T. Dean,⁵³ D. Decamp,⁴ L. Del Buono,⁸ B. Delaney,⁴⁹ H.-P. Dembinski,¹¹ M. Demmer,¹⁰ A. Dendek,³⁰ D. Derkach,³⁷ O. Deschamps,⁵ F. Desse,⁷ F. Dettori,⁵⁴ B. Dey,⁶⁵ A. Di Canto,⁴² P. Di Nezza,¹⁸ S. Didenko,⁷⁰ H. Dijkstra,⁴² F. Dordei,⁴² M. Dorigo,^{42,k} A. Dosil Suárez,⁴¹ L. Douglas,⁵³ A. Dovbnya,⁴⁵ K. Dreimanis,⁵⁴ L. Dufour,²⁷ G. Dujany,⁸ P. Durante,⁴² J. M. Durham,⁷⁴ D. Dutta,⁵⁶ R. Dzhelezhyan,³⁹ M. Dziewiecki,¹² A. Dziurda,²⁹ A. Dzyuba,³³ S. Easo,⁵¹ U. Egede,⁵⁵ V. Egorychev,³⁴ S. Eidelman,^{38,e} S. Eisenhardt,⁵² U. Eitschberger,¹⁰ R. Ekelhof,¹⁰ L. Eklund,⁵³ S. Ely,⁶¹ A. Ene,³² S. Escher,⁹ S. Esen,²⁷ T. Evans,⁵⁹ A. Falabella,¹⁵ N. Farley,⁴⁷ S. Farry,⁵⁴ D. Fazzini,^{20,42,c} L. Federici,²⁵ P. Fernandez Declara,⁴² A. Fernandez Prieto,⁴¹ F. Ferrari,¹⁵ L. Ferreira Lopes,⁴³ F. Ferreira Rodrigues,² M. Ferro-Luzzi,⁴² S. Filippov,³⁶ R. A. Fini,¹⁴ M. Fiorini,^{16,a} M. Firlej,³⁰ C. Fitzpatrick,⁴³ T. Fiutowski,³⁰ F. Fleuret,^{7,b} M. Fontana,^{22,42} F. Fontanelli,^{19,h} R. Forty,⁴² V. Franco Lima,⁵⁴ M. Frank,⁴² C. Frei,⁴² J. Fu,^{21,l} W. Funk,⁴² C. Färber,⁴² M. Féo Pereira Rivello Carvalho,²⁷ E. Gabriel,⁵² A. Gallas Torreira,⁴¹ D. Galli,^{15,g} S. Gallorini,²³ S. Gambetta,⁵² Y. Gan,³

M. Gandelman,² P. Gandini,²¹ Y. Gao,³ L. M. Garcia Martin,⁷² B. Garcia Plana,⁴¹ J. García Pardiñas,⁴⁴ J. Garra Tico,⁴⁹ L. Garrido,⁴⁰ D. Gascon,⁴⁰ C. Gaspar,⁴² L. Gavardi,¹⁰ G. Gazzoni,⁵ D. Gerick,¹² E. Gersabeck,⁵⁶ M. Gersabeck,⁵⁶ T. Gershon,⁵⁰ D. Gerstel,⁶ Ph. Ghez,⁴ S. Giani,⁴³ V. Gibson,⁴⁹ O. G. Girard,⁴³ L. Giubega,³² K. Gizdov,⁵² V. V. Gligorov,⁸ D. Golubkov,³⁴ A. Golutvin,^{55,70} A. Gomes,^{1,m} I. V. Gorelov,³⁵ C. Gotti,^{20,c} E. Govorkova,²⁷ J. P. Grabowski,¹² R. Graciani Diaz,⁴⁰ L. A. Granado Cardoso,⁴² E. Graugés,⁴⁰ E. Graverini,⁴⁴ G. Graziani,¹⁷ A. Greco,³² R. Greim,²⁷ P. Griffith,²² L. Grillo,⁵⁶ L. Gruber,⁴² B. R. Gruberg Cazon,⁵⁷ O. Grünberg,⁶⁷ C. Gu,³ E. Gushchin,³⁶ Yu. Guz,^{39,42} T. Gys,⁴² C. Göbel,⁶² T. Hadavizadeh,⁵⁷ C. Hadjivasiliou,⁵ G. Haefeli,⁴³ C. Haen,⁴² S. C. Haines,⁴⁹ B. Hamilton,⁶⁰ X. Han,¹² T. H. Hancock,⁵⁷ S. Hansmann-Menzemer,¹² N. Harnew,⁵⁷ S. T. Harnew,⁴⁸ T. Harrison,⁵⁴ C. Hasse,⁴² M. Hatch,⁴² J. He,⁶³ M. Hecker,⁵⁵ K. Heinicke,¹⁰ A. Heister,¹⁰ K. Hennessy,⁵⁴ L. Henry,⁷² E. van Herwijnen,⁴² M. Heß,⁶⁷ A. Hicheur,² R. Hidalgo Charman,⁵⁶ D. Hill,⁵⁷ M. Hilton,⁵⁶ P. H. Hopchev,⁴³ W. Hu,⁶⁵ W. Huang,⁶³ Z. C. Huard,⁵⁹ W. Hulsbergen,²⁷ T. Humair,⁵⁵ M. Hushchyn,³⁷ D. Hutchcroft,⁵⁴ D. Hynds,²⁷ P. Ibis,¹⁰ M. Idzik,³⁰ P. Ilten,⁴⁷ K. Ivshin,³³ R. Jacobsson,⁴² J. Jalocha,⁵⁷ E. Jans,²⁷ A. Jawahery,⁶⁰ F. Jiang,³ M. John,⁵⁷ D. Johnson,⁴² C. R. Jones,⁴⁹ C. Joram,⁴² B. Jost,⁴² N. Jurik,⁵⁷ S. Kandybei,⁴⁵ M. Karacson,⁴² J. M. Kariuki,⁴⁸ S. Karodia,⁵³ N. Kazeev,³⁷ M. Kecke,¹² F. Keizer,⁴⁹ M. Kelsey,⁶¹ M. Kenzie,⁴⁹ T. Ketel,²⁸ E. Khairullin,³⁷ B. Khanji,¹² C. Khurewathanakul,⁴³ K. E. Kim,⁶¹ T. Kirn,⁹ S. Klaver,¹⁸ K. Klimaszewski,³¹ T. Klimkovich,¹¹ S. Koliiev,⁴⁶ M. Kolpin,¹² R. Kopecna,¹² P. Koppenburg,²⁷ I. Kostiuik,²⁷ S. Kotriakhova,³³ M. Kozeiha,⁵ L. Kravchuk,³⁶ M. Kreps,⁵⁰ F. Kress,⁵⁵ P. Krokovny,^{38,e} W. Krupa,³⁰ W. Krzemien,³¹ W. Kucewicz,^{29,n} M. Kucharczyk,²⁹ V. Kudryavtsev,^{38,e} A. K. Kuonen,⁴³ T. Kvaratskheliya,^{34,42} D. Lacarrere,⁴² G. Lafferty,⁵⁶ A. Lai,²² D. Lancierini,⁴⁴ G. Lanfranchi,¹⁸ C. Langenbruch,⁹ T. Latham,⁵⁰ C. Lazzeroni,⁴⁷ R. Le Gac,⁶ A. Leflat,³⁵ J. Lefrançois,⁷ R. Lefèvre,⁵ F. Lemaître,⁴² O. Leroy,⁶ T. Lesiak,²⁹ B. Leverington,¹² P.-R. Li,⁶³ T. Li,³ Z. Li,⁶¹ X. Liang,⁶¹ T. Likhomanenko,⁶⁹ R. Lindner,⁴² F. Lionetto,⁴⁴ V. Lisovskyi,⁷ X. Liu,³ D. Loh,⁵⁰ A. Loi,²² I. Longstaff,⁵³ J. H. Lopes,² G. H. Lovell,⁴⁹ D. Lucchesi,^{23,p} M. Lucio Martinez,⁴¹ A. Lupato,²³ E. Luppi,^{16,a} O. Lupton,⁴² A. Lusiani,²⁴ X. Lyu,⁶³ F. Machefert,⁷ F. Maciuc,³² V. Macko,⁴³ P. Mackowiak,¹⁰ S. Maddrell-Mander,⁴⁸ O. Maev,^{33,42} K. Maguire,⁵⁶ D. Maisuzenko,³³ M. W. Majewski,³⁰ S. Malde,⁵⁷ B. Malecki,²⁹ A. Malinin,⁶⁹ T. Maltsev,^{38,e} G. Manca,^{22,q} G. Mancinelli,⁶ D. Marangotto,^{21,l} J. Maratas,^{5,r} J. F. Marchand,⁴ U. Marconi,¹⁵ C. Marin Benito,⁷ M. Marinangeli,⁴³ P. Marino,⁴³ J. Marks,¹² P. J. Marshall,⁵⁴ G. Martellotti,²⁶ M. Martin,⁶ M. Martinelli,⁴² D. Martinez Santos,⁴¹ F. Martinez Vidal,⁷² A. Massafferri,¹ M. Materok,⁹ R. Matev,⁴² A. Mathad,⁵⁰ Z. Mathe,⁴² C. Matteuzzi,²⁰ A. Mauri,⁴⁴ E. Maurice,^{7,b} B. Maurin,⁴³ A. Mazurov,⁴⁷ M. McCann,^{55,42} A. McNab,⁵⁶ R. McNulty,¹³ J. V. Mead,⁵⁴ B. Meadows,⁵⁹ C. Meaux,⁶ F. Meier,¹⁰ N. Meinert,⁶⁷ D. Melnychuk,³¹ M. Merk,²⁷ A. Merli,^{21,l} E. Michielin,²³ D. A. Milanes,⁶⁶ E. Millard,⁵⁰ M.-N. Minard,⁴ L. Minzoni,^{16,a} D. S. Mitzel,¹² A. Mogini,⁸ J. Molina Rodriguez,^{1,s} T. Mombächer,¹⁰ I. A. Monroy,⁶⁶ S. Monteil,⁵ M. Morandin,²³ G. Morello,¹⁸ M. J. Morello,^{24,t} O. Morgunova,⁶⁹ J. Moron,³⁰ A. B. Morris,⁶ R. Mountain,⁶¹ F. Muheim,⁵² M. Mulder,²⁷ C. H. Murphy,⁵⁷ D. Murray,⁵⁶ A. Mödden,¹⁰ D. Müller,⁴² J. Müller,¹⁰ K. Müller,⁴⁴ V. Müller,¹⁰ P. Naik,⁴⁸ T. Nakada,⁴³ R. Nandakumar,⁵¹ A. Nandi,⁵⁷ T. Nanut,⁴³ I. Nasteva,² M. Needham,⁵² N. Neri,²¹ S. Neubert,¹² N. Neufeld,⁴² M. Neuner,¹² T. D. Nguyen,⁴³ C. Nguyen-Mau,^{43,u} S. Nieswand,⁹ R. Niet,¹⁰ N. Nikitin,³⁵ A. Nogay,⁶⁹ N. S. Nolte,⁴² D. P. O'Hanlon,¹⁵ A. Oblakowska-Mucha,³⁰ V. Obraztsov,³⁹ S. Ogilvy,¹⁸ R. Oldeman,^{22,q} C. J. G. Onderwater,⁶⁸ A. Ossowska,²⁹ J. M. Otalora Goicochea,² P. Owen,⁴⁴ A. Oyanguren,⁷² P. R. Pais,⁴³ T. Pajero,^{24,t} A. Palano,¹⁴ M. Palutan,^{18,42} G. Panshin,⁷¹ A. Papanestis,⁵¹ M. Pappagallo,⁵² L. L. Pappalardo,^{16,a} W. Parker,⁶⁰ C. Parkes,⁵⁶ G. Passaleva,^{17,42} A. Pastore,¹⁴ M. Patel,⁵⁵ C. Patrignani,^{15,g} A. Pearce,⁴² A. Pellegrino,²⁷ G. Penso,²⁶ M. Pepe Altarelli,⁴² S. Perazzini,⁴² D. Pereima,³⁴ P. Perret,⁵ L. Pescatore,⁴³ K. Petridis,⁴⁸ A. Petrolini,^{19,h} A. Petrov,⁶⁹ S. Petrucci,⁵² M. Petruzzio,^{21,l} B. Pietrzyk,⁴ G. Pietrzyk,⁴³ M. Pikies,²⁹ M. Pili,⁵⁷ D. Pinci,²⁶ J. Pinzino,⁴² F. Pisani,^{42,o} A. Piucci,¹² V. Placinta,³² S. Playfer,⁵² J. Plews,⁴⁷ M. Plo Casasus,⁴¹ F. Polci,⁸ M. Poli Lener,¹⁸ A. Poluektov,⁵⁰ N. Polukhina,^{70,v} I. Polyakov,⁶¹ E. Polcarpo,² G. J. Pomery,⁴⁸ S. Ponce,⁴² A. Popov,³⁹ D. Popov,^{47,11} S. Poslavskii,³⁹ C. Potterat,² E. Price,⁴⁸ J. Prisciandaro,⁴¹ C. Prouve,⁴⁸ V. Pugatch,⁴⁶ A. Puig Navarro,⁴⁴ H. Pullen,⁵⁷ G. Punzi,^{24,i} W. Qian,⁶³ J. Qin,⁶³ R. Quagliani,⁸ B. Quintana,⁵ B. Rachwal,³⁰ J. H. Rademacker,⁴⁸ M. Rama,²⁴ M. Ramos Pernas,⁴¹ M. S. Rangel,² F. Ratnikov,^{37,w} G. Raven,²⁸ M. Ravonel Salzgeber,⁴² M. Reboud,⁴ F. Redi,⁴³ S. Reichert,¹⁰ A. C. dos Reis,¹ F. Reiss,⁸ C. Remon Alepuz,⁷² Z. Ren,³ V. Renaudin,⁷ S. Ricciardi,⁵¹ S. Richards,⁴⁸ K. Rinnert,⁵⁴ P. Robbe,⁷ A. Robert,⁸ A. B. Rodrigues,⁴³ E. Rodrigues,⁵⁹ J. A. Rodriguez Lopez,⁶⁶ M. Roehrken,⁴² A. Rogozhnikov,³⁷ S. Roiser,⁴² A. Rollings,⁵⁷ V. Romanovskiy,³⁹ A. Romero Vidal,⁴¹ M. Rotondo,¹⁸ M. S. Rudolph,⁶¹ T. Ruf,⁴² J. Ruiz Vidal,⁷² J. J. Saborido Silva,⁴¹ N. Sagidova,³³ B. Saitta,^{22,q} V. Salustino Guimaraes,⁶² C. Sanchez Gras,²⁷ C. Sanchez Mayordomo,⁷² B. Sanmartin Sedes,⁴¹ R. Santacesaria,²⁶ C. Santamarina Rios,⁴¹ M. Santimaria,¹⁸ E. Santovetti,^{25,x} G. Sarpis,⁵⁶ A. Sarti,^{18,y} C. Satriano,^{26,z}

A. Satta,²⁵ M. Saur,⁶³ D. Savrina,^{34,35} S. Schael,⁹ M. Schellenberg,¹⁰ M. Schiller,⁵³ H. Schindler,⁴² M. Schmelling,¹¹ T. Schmelzer,¹⁰ B. Schmidt,⁴² O. Schneider,⁴³ A. Schopper,⁴² H. F. Schreiner,⁵⁹ M. Schubiger,⁴³ M. H. Schune,⁷ R. Schwemmer,⁴² B. Sciascia,¹⁸ A. Sciubba,^{26,y} A. Semennikov,³⁴ E. S. Sepulveda,⁸ A. Sergi,^{47,42} N. Serra,⁴⁴ J. Serrano,⁶ L. Sestini,²³ A. Seuthe,¹⁰ P. Seyfert,⁴² M. Shapkin,³⁹ Y. Shcheglov,³³ T. Shears,⁵⁴ L. Shekhtman,^{38,e} V. Shevchenko,⁶⁹ E. Shmanin,⁷⁰ B. G. Siddi,¹⁶ R. Silva Coutinho,⁴⁴ L. Silva de Oliveira,² G. Simi,^{23,p} S. Simone,^{14,j} N. Skidmore,¹² T. Skwarnicki,⁶¹ J. G. Smeaton,⁴⁹ E. Smith,⁹ I. T. Smith,⁵² M. Smith,⁵⁵ M. Soares,¹⁵ I. Soares Lavra,¹ M. D. Sokoloff,⁵⁹ F. J. P. Soler,⁵³ B. Souza De Paula,² B. Spaan,¹⁰ P. Spradlin,⁵³ F. Stagni,⁴² M. Stahl,¹² S. Stahl,⁴² P. Stefko,⁴³ S. Stefkova,⁵⁵ O. Steinkamp,⁴⁴ S. Stemmle,¹² O. Stenyakin,³⁹ M. Stepanova,³³ H. Stevens,¹⁰ A. Stocchi,⁷ S. Stone,⁶¹ B. Storaci,⁴⁴ S. Stracka,^{24,i} M. E. Stramaglia,⁴³ M. Straticiu,³² U. Straumann,⁴⁴ S. Strovkov,⁷¹ J. Sun,³ L. Sun,⁶⁴ K. Swientek,³⁰ V. Syropoulos,²⁸ T. Szumlak,³⁰ M. Szymanski,⁶³ S. T'Jampens,⁴ Z. Tang,³ A. Tayduganov,⁶ T. Tekampe,¹⁰ G. Tellarini,¹⁶ F. Teubert,⁴² E. Thomas,⁴² J. van Tilburg,²⁷ M. J. Tilley,⁵⁵ V. Tisserand,⁵ M. Tobin,³⁰ S. Tolk,⁴² L. Tomassetti,^{16,a} D. Tonelli,²⁴ D. Y. Tou,⁸ R. Tourinho Jadallah Aoude,¹ E. Tournefier,⁴ M. Traill,⁵³ M. T. Tran,⁴³ A. Trisovic,⁴⁹ A. Tsaregorodtsev,⁶ G. Tuci,²⁴ A. Tully,⁴⁹ N. Tuning,^{27,42} A. Ukleja,³¹ A. Usachov,⁷ A. Ustyuzhanin,³⁷ U. Uwer,¹² A. Vagner,⁷¹ V. Vagnoni,¹⁵ A. Valassi,⁴² S. Valat,⁴² G. Valenti,¹⁵ R. Vazquez Gomez,⁴² P. Vazquez Regueiro,⁴¹ S. Vecchi,¹⁶ M. van Veghel,²⁷ J. J. Velthuis,⁴⁸ M. Veltri,^{17,aa} G. Veneziano,⁵⁷ A. Venkateswaran,⁶¹ T. A. Verlage,⁹ M. Vernet,⁵ M. Veronesi,²⁷ N. V. Veronika,¹³ M. Vesterinen,⁵⁷ J. V. Viana Barbosa,⁴² D. Vieira,⁶³ M. Vieites Diaz,⁴¹ H. Viemann,⁶⁷ X. Vilasis-Cardona,^{40,f} A. Vitkovskiy,²⁷ M. Vitti,⁴⁹ V. Volkov,³⁵ A. Vollhardt,⁴⁴ B. Voneki,⁴² A. Vorobyev,³³ V. Vorobyev,^{38,e} J. A. de Vries,²⁷ C. Vázquez Sierra,²⁷ R. Waldi,⁶⁷ J. Walsh,²⁴ J. Wang,⁶¹ M. Wang,³ Y. Wang,⁶⁵ Z. Wang,⁴⁴ D. R. Ward,⁴⁹ H. M. Wark,⁵⁴ N. K. Watson,⁴⁷ D. Websdale,⁵⁵ A. Weiden,⁴⁴ C. Weisser,⁵⁸ M. Whitehead,⁹ J. Wicht,⁵⁰ G. Wilkinson,⁵⁷ M. Wilkinson,⁶¹ I. Williams,⁴⁹ M. R. J. Williams,⁵⁶ M. Williams,⁵⁸ T. Williams,⁴⁷ F. F. Wilson,^{51,42} J. Wimberley,⁶⁰ M. Winn,⁷ J. Wishahi,¹⁰ W. Wislicki,³¹ M. Witek,²⁹ G. Wormser,⁷ S. A. Wotton,⁴⁹ K. Wyllie,⁴² D. Xiao,⁶⁵ Y. Xie,⁶⁵ A. Xu,³ M. Xu,⁶⁵ Q. Xu,⁶³ Z. Xu,³ Z. Xu,⁴ Z. Yang,³ Z. Yang,⁶⁰ Y. Yao,⁶¹ L. E. Yeomans,⁵⁴ H. Yin,⁶⁵ J. Yu,^{65,bb} X. Yuan,⁶¹ O. Yushchenko,³⁹ K. A. Zarebski,⁴⁷ M. Zavertyaev,^{11,v} D. Zhang,⁶⁵ L. Zhang,³ W. C. Zhang,^{3,cc} Y. Zhang,⁷ A. Zhelezov,¹² Y. Zheng,⁶³ X. Zhu,³ V. Zhukov,^{9,35} J. B. Zonneveld,⁵² and S. Zucchelli¹⁵

(LHCb Collaboration)

¹Centro Brasileiro de Pesquisas Físicas (CBPF), Rio de Janeiro, Brazil²Universidade Federal do Rio de Janeiro (UFRJ), Rio de Janeiro, Brazil³Center for High Energy Physics, Tsinghua University, Beijing, China⁴Univ. Grenoble Alpes, Univ. Savoie Mont Blanc, CNRS, IN2P3-LAPP, Annecy, France⁵Clermont Université, Université Blaise Pascal, CNRS/IN2P3, LPC, Clermont-Ferrand, France⁶Aix Marseille Univ, CNRS/IN2P3, CPPM, Marseille, France⁷LAL, Univ. Paris-Sud, CNRS/IN2P3, Université Paris-Saclay, Orsay, France⁸LPNHE, Sorbonne Université, Paris Diderot Sorbonne Paris Cité, CNRS/IN2P3, Paris, France⁹I. Physikalisches Institut, RWTH Aachen University, Aachen, Germany¹⁰Fakultät Physik, Technische Universität Dortmund, Dortmund, Germany¹¹Max-Planck-Institut für Kernphysik (MPIK), Heidelberg, Germany¹²Physikalisches Institut, Ruprecht-Karls-Universität Heidelberg, Heidelberg, Germany¹³School of Physics, University College Dublin, Dublin, Ireland¹⁴INFN Sezione di Bari, Bari, Italy¹⁵INFN Sezione di Bologna, Bologna, Italy¹⁶INFN Sezione di Ferrara, Ferrara, Italy¹⁷INFN Sezione di Firenze, Firenze, Italy¹⁸INFN Laboratori Nazionali di Frascati, Frascati, Italy¹⁹INFN Sezione di Genova, Genova, Italy²⁰INFN Sezione di Milano-Bicocca, Milano, Italy²¹INFN Sezione di Milano, Milano, Italy²²INFN Sezione di Cagliari, Monserrato, Italy²³INFN Sezione di Padova, Padova, Italy²⁴INFN Sezione di Pisa, Pisa, Italy²⁵INFN Sezione di Roma Tor Vergata, Roma, Italy²⁶INFN Sezione di Roma La Sapienza, Roma, Italy

- ²⁷*Nikhef National Institute for Subatomic Physics, Amsterdam, Netherlands*
- ²⁸*Nikhef National Institute for Subatomic Physics and VU University Amsterdam, Amsterdam, Netherlands*
- ²⁹*Henryk Niewodniczanski Institute of Nuclear Physics Polish Academy of Sciences, Kraków, Poland*
- ³⁰*AGH—University of Science and Technology, Faculty of Physics and Applied Computer Science, Kraków, Poland*
- ³¹*National Center for Nuclear Research (NCBJ), Warsaw, Poland*
- ³²*Horia Hulubei National Institute of Physics and Nuclear Engineering, Bucharest-Magurele, Romania*
- ³³*Petersburg Nuclear Physics Institute (PNPI), Gatchina, Russia*
- ³⁴*Institute of Theoretical and Experimental Physics (ITEP), Moscow, Russia*
- ³⁵*Institute of Nuclear Physics, Moscow State University (SINP MSU), Moscow, Russia*
- ³⁶*Institute for Nuclear Research of the Russian Academy of Sciences (INR RAS), Moscow, Russia*
- ³⁷*Yandex School of Data Analysis, Moscow, Russia*
- ³⁸*Budker Institute of Nuclear Physics (SB RAS), Novosibirsk, Russia*
- ³⁹*Institute for High Energy Physics (IHEP), Protvino, Russia*
- ⁴⁰*ICCUB, Universitat de Barcelona, Barcelona, Spain*
- ⁴¹*Instituto Galego de Física de Altas Enerxías (IGFAE), Universidade de Santiago de Compostela, Santiago de Compostela, Spain*
- ⁴²*European Organization for Nuclear Research (CERN), Geneva, Switzerland*
- ⁴³*Institute of Physics, Ecole Polytechnique Fédérale de Lausanne (EPFL), Lausanne, Switzerland*
- ⁴⁴*Physik-Institut, Universität Zürich, Zürich, Switzerland*
- ⁴⁵*NSC Kharkiv Institute of Physics and Technology (NSC KIPT), Kharkiv, Ukraine*
- ⁴⁶*Institute for Nuclear Research of the National Academy of Sciences (KINR), Kyiv, Ukraine*
- ⁴⁷*University of Birmingham, Birmingham, United Kingdom*
- ⁴⁸*H.H. Wills Physics Laboratory, University of Bristol, Bristol, United Kingdom*
- ⁴⁹*Cavendish Laboratory, University of Cambridge, Cambridge, United Kingdom*
- ⁵⁰*Department of Physics, University of Warwick, Coventry, United Kingdom*
- ⁵¹*STFC Rutherford Appleton Laboratory, Didcot, United Kingdom*
- ⁵²*School of Physics and Astronomy, University of Edinburgh, Edinburgh, United Kingdom*
- ⁵³*School of Physics and Astronomy, University of Glasgow, Glasgow, United Kingdom*
- ⁵⁴*Oliver Lodge Laboratory, University of Liverpool, Liverpool, United Kingdom*
- ⁵⁵*Imperial College London, London, United Kingdom*
- ⁵⁶*School of Physics and Astronomy, University of Manchester, Manchester, United Kingdom*
- ⁵⁷*Department of Physics, University of Oxford, Oxford, United Kingdom*
- ⁵⁸*Massachusetts Institute of Technology, Cambridge, Massachusetts, USA*
- ⁵⁹*University of Cincinnati, Cincinnati, Ohio, USA*
- ⁶⁰*University of Maryland, College Park, Maryland, USA*
- ⁶¹*Syracuse University, Syracuse, New York, USA*
- ⁶²*Pontifícia Universidade Católica do Rio de Janeiro (PUC-Rio), Rio de Janeiro, Brazil
(associated with Universidade Federal do Rio de Janeiro (UFRJ), Rio de Janeiro, Brazil)*
- ⁶³*University of Chinese Academy of Sciences, Beijing, China
(associated with Center for High Energy Physics, Tsinghua University, Beijing, China)*
- ⁶⁴*School of Physics and Technology, Wuhan University, Wuhan, China
(associated with Center for High Energy Physics, Tsinghua University, Beijing, China)*
- ⁶⁵*Institute of Particle Physics, Central China Normal University, Wuhan, Hubei, China
(associated with Center for High Energy Physics, Tsinghua University, Beijing, China)*
- ⁶⁶*Departamento de Física, Universidad Nacional de Colombia, Bogota, Colombia
(associated with LPNHE, Sorbonne Université, Paris Diderot Sorbonne Paris Cité, CNRS/IN2P3, Paris, France)*
- ⁶⁷*Institut für Physik, Universität Rostock, Rostock, Germany
(associated with Physikalisches Institut, Ruprecht-Karls-Universität Heidelberg, Heidelberg, Germany)*
- ⁶⁸*Van Swinderen Institute, University of Groningen, Groningen, Netherlands
(associated with Nikhef National Institute for Subatomic Physics, Amsterdam, Netherlands)*
- ⁶⁹*National Research Centre Kurchatov Institute, Moscow, Russia
(associated with Institute of Theoretical and Experimental Physics (ITEP), Moscow, Russia)*
- ⁷⁰*National University of Science and Technology “MISIS”, Moscow, Russia
(associated with Institute of Theoretical and Experimental Physics (ITEP), Moscow, Russia)*
- ⁷¹*National Research Tomsk Polytechnic University, Tomsk, Russia
(associated with Institute of Theoretical and Experimental Physics (ITEP), Moscow, Russia)*
- ⁷²*Instituto de Física Corpuscular, Centro Mixto Universidad de Valencia—CSIC, Valencia, Spain
(associated with ICCUB, Universitat de Barcelona, Barcelona, Spain)*
- ⁷³*University of Michigan, Ann Arbor, USA
(associated with Syracuse University, Syracuse, New York, USA)*

⁷⁴*Los Alamos National Laboratory (LANL), Los Alamos, USA
(associated with Syracuse University, Syracuse, New York, USA)*

^aAlso at Università di Ferrara, Ferrara, Italy.

^bAlso at Laboratoire Leprince-Ringuet, Palaiseau, France.

^cAlso at Università di Milano Bicocca, Milano, Italy.

^dAlso at Università di Modena e Reggio Emilia, Modena, Italy.

^eAlso at Novosibirsk State University, Novosibirsk, Russia.

^fAlso at LIFAELS, La Salle, Universitat Ramon Llull, Barcelona, Spain.

^gAlso at Università di Bologna, Bologna, Italy.

^hAlso at Università di Genova, Genova, Italy.

ⁱAlso at Università di Pisa, Pisa, Italy.

^jAlso at Università di Bari, Bari, Italy.

^kAlso at Sezione INFN di Trieste, Trieste, Italy.

^lAlso at Università degli Studi di Milano, Milano, Italy.

^mAlso at Universidade Federal do Triângulo Mineiro (UFTM), Uberaba-MG, Brazil.

ⁿAlso at AGH—University of Science and Technology, Faculty of Computer Science, Electronics and Telecommunications, Kraków, Poland.

^oAlso at INFN Sezione di Bologna, Bologna, Italy

^pAlso at Università di Padova, Padova, Italy.

^qAlso at Università di Cagliari, Cagliari, Italy.

^rAlso at MSU—Iligan Institute of Technology (MSU-IIT), Iligan, Philippines.

^sAlso at Escuela Agrícola Panamericana, San Antonio de Oriente, Honduras.

^tAlso at Scuola Normale Superiore, Pisa, Italy.

^uAlso at Hanoi University of Science, Hanoi, Vietnam.

^vAlso at P.N. Lebedev Physical Institute, Russian Academy of Science (LPI RAS), Moscow, Russia.

^wAlso at National Research University Higher School of Economics, Moscow, Russia.

^xAlso at Università di Roma Tor Vergata, Roma, Italy.

^yAlso at Università di Roma La Sapienza, Roma, Italy.

^zAlso at Università della Basilicata, Potenza, Italy.

^{aa}Also at Università di Urbino, Urbino, Italy.

^{bb}Also at Physics and Micro Electronic College, Hunan University, Changsha City, China.

^{cc}Also at School of Physics and Information Technology, Shaanxi Normal University (SNNU), Xi'an, China.